J. Fac. Cul. Edu. Saga Univ.
Vol. 5, No. 1 (2000) 237~244

ab Initio MO Study on the Solvent Effect for S_N2 Type Nucleophilic Ring Opening of Aflatoxin B_1 8,9-Oxide

Toshiya OKAJIMA* and Akane HASHIKAWA

Abstract:

ab Initio MO calculation was performed to study the solvent effect for S_N2 type nucleophilic oxirane ring opening of aflatoxin B_1 8,9-oxide by using model compounds, (*2S, 3R, 3aR, 6aS*) - 3a, 6a -dihydrofuro [2, 3-*b*] furan 2,3-oxide (**I**) and (*2R, 3S, 3aR, 6aS*) - 3a, 6a -dihydrofuro [2, 3-*b*] furan 2,3-oxide (**II**). Two and three H_2O molecules were considered for the solvation to oxirane oxygen, on which negative charge grows as the reaction proceeds. Stationary points including transition structures (**TSs**) were optimized with no geometrical constraint at the RHF/3-21G basis set. The activation energies ($\Delta E^{\neq}$) were evaluated at Becke3LYP/3-21G level based on the RHF/3-21G geometries. Calculation clarified that (1) involvement of the solvent molecules accelerate the reaction, (2) endo-attacking process is more favorable than exo-attacking one ($\Delta E^{\neq}$ values are +24.4 kcal/mol (**TS-I**), +9.7 (**TS-I$_2$**), and +7.4 (**TS-I$_3$**)) for the reaction of **I** and +32.2 (**TS-II**), +14.3 (**TS-II$_2$-ob**), and +20.5 (**TS-II$_3$**)) for **II**, (3) for endo-attacking TSs, $\Delta E^{\neq}$ value of **TS-I$_3$** (+7.4kcal/mol) coordinated by three H_2O molecules is the smallest, while **TS-II$_2$-ob** with two H_2O molecules has the smallest $\Delta E^{\neq}$ value in the series of exo attacking TSs, and (4) for exo-attacking TSs, steric hindrance for solvent coordination increases in the order of outside (o) < backside (b) < inside (i) position.

Introduction

Aflatoxin B_1 (AFB_1) is one of the most potent mutagens involved in human carcinogenesis.[1] Aflatoxins, which belong to a group of dihydrofurans, are produced by the fungal molds *Aspergillus flavus, A. parasiticus*, and *A. nomius* ,[2] and is much interested in health science. AFB_1 exo-8,9-oxide (**1**), which is produced by the metabolic activation of AFB_1 mainly by the liver enzyme cytochrome P450,[3] is known to be a very reactive electrophile, which forms adducts by the reaction with guanine at N7 position in DNA (genotoxic) (Chart 1).[4] On the other hand, the endo oxide is known to be unreactive with DNA, and therefore, it is essentially nongenotoxic stereoisomer.[5] To investigate the toxicity of AFB_1 8,9-oxide, some theoretical calculation[6] on the ground state structures including intercalation, DNA adduct conformation,[6a] and frontier orbital analysis[6b] were performed. However, no study on the transition structure (TS) for nucleophilic oxirane ring opening, resulting in the covalent bonding of **1** to nucleic acid bases, is found. In this study, the solvent effect for the transition structures of S_N2 type nucleophilic oxirane ring opening of the model compounds (**I** and **II**) have been investigated. Model compounds **I** and **II** include only furofurano ring (A and B ring) in **1**. The anti configuration between oxirane ring and B ring with respective to A ring is designated as exo and syn as endo (Chart 1).

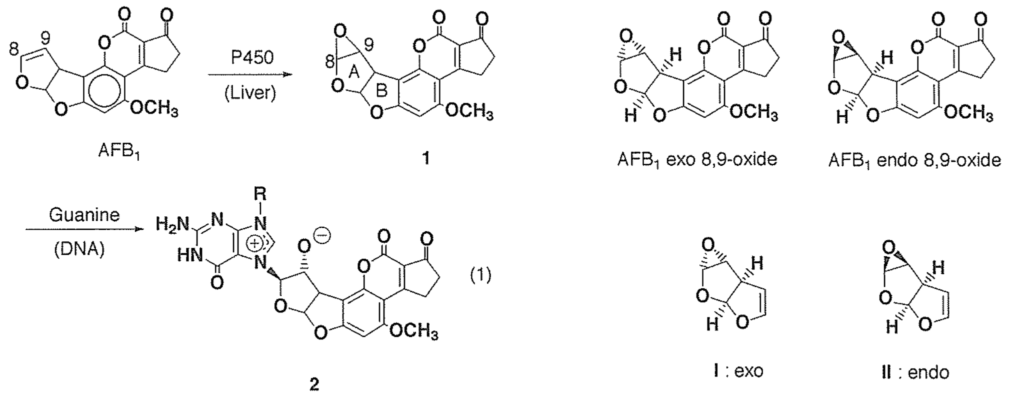

Chart 1

Method

ab Initio molecular orbital calculation was performed using GAUSSIAN 98 programs.[7] Geometries of all stationary points including transition structures (TSs) were optimized utilizing gradient method without any geometrical constraint at the RHF/3-21G basis set. Activation energies ($\Delta E^{\neq}$) were evaluated at Becke3LYP/3-21G level of theory based on the RHF/3-21G geometries.[8] All TSs were tested by frequency analysis and some by IRC calculation.[9] For stationary points, an energy minimum (reactant) and maximum point (TS) were characterized by the correct number of negative eigenvalue of their Hessian matrix, that is, the former and the latter have no and a single imaginary frequency, respectively.

Results and Discussion

Fig. 1 shows RHF/3-21G TSs (**TS-I** and **TS-II**) and the corresponding initial complexes (**IC-I** and **IC-II**, respectively) for S_N2 type nucleophilic reaction by NH_3 molecule to oxirane carbon. **IC-I** and **IC-II** have the structures that NH_3 molecule coordinates to oxirane oxygen. Activation energies ($\Delta E^{\neq}$, Becke3LYP/3-21G//RHF/3-21G)[10] are +24.4 kcal/mol for endo-attacking process (**TS-I**) and +32.2 for exo-attacking one (**TS-II**). Since energy difference between **IC-I** and **IC-II** is only 0.9 kcal/mol (**IC-I** is more stable), the difference of $\Delta E^{\neq}$ values can be mainly attributable to that (8.7 kcal/mol) between two TSs. This is maybe because of favorable Coulomb interaction between ethereal oxygen in B ring and positively charged proton of NH_3 in **TS-I** and

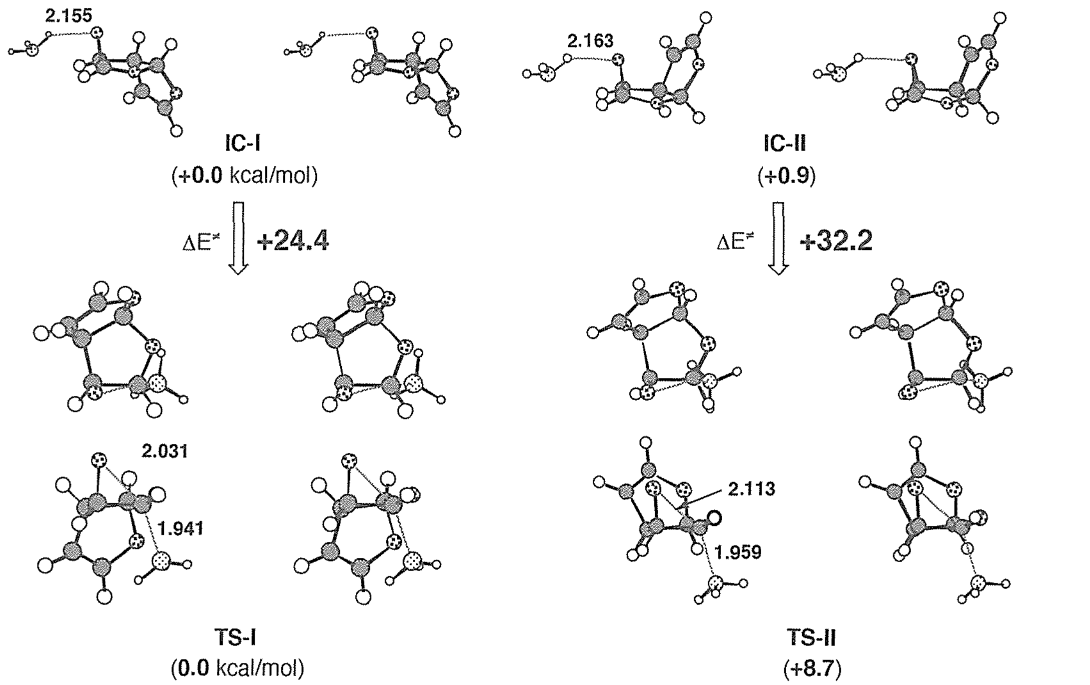

Fig.1 Stereoviews of RHF/3-21G transition structures (**TS- I** and **TS-II**) and the corresponding initial complexes (**IC- I** and **IC-II**, respectively) for S_N2 type nucleophilic oxirane ring opening by NH_3. No solvent molecules are considered. Atomic distances are in angstroms. Energy differences (in kcal/mol) are at Becke3LYP/3-21G//RHF/3-21G level of theory.

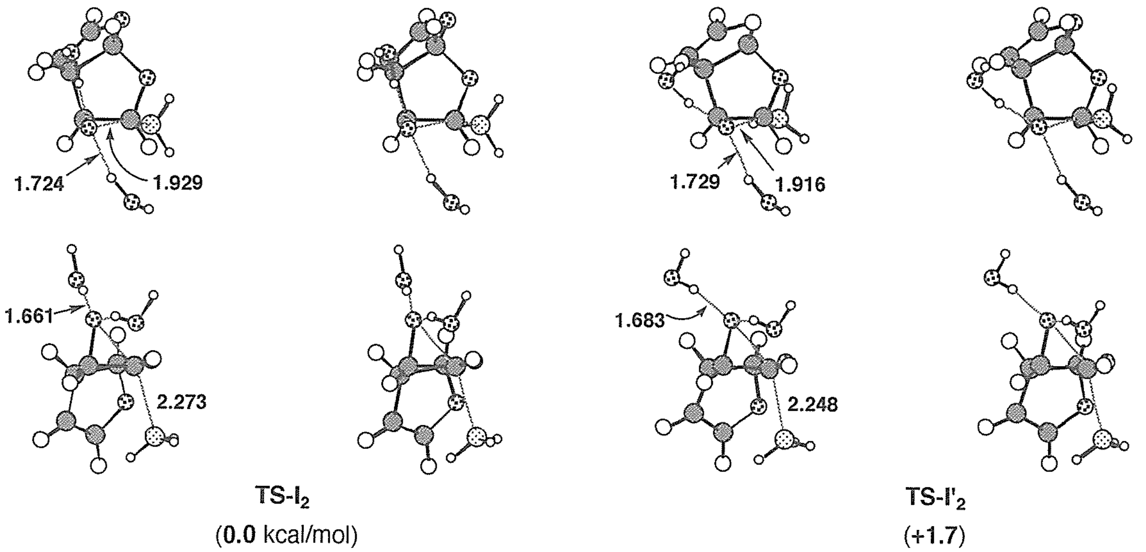

Fig.2 Stereoviews of RHF/3-21G transition structures for S_N2 type nucleophilic oxirane ring opening of exo type model compound (**I**) by NH_3 molecule. Two H_2O molecules coordinate to oxirane oxygen, on which negative charge grows as the reaction proceeds. Two types of coordinating geometries could be located, which are designated as **TS- I** $_2$, **TS-II** $'_2$. Atomic distances are in angstroms. Energy differences are at Becke3LYP/3-21G//RHF/3-21G.

unfavorable repulsive Coulomb interaction between negatively charged oxirane oxygen and the facing electron-rich B ring in **TS-II**. The difference of $\Delta E^{\neq}$s of these two TSs calculated at

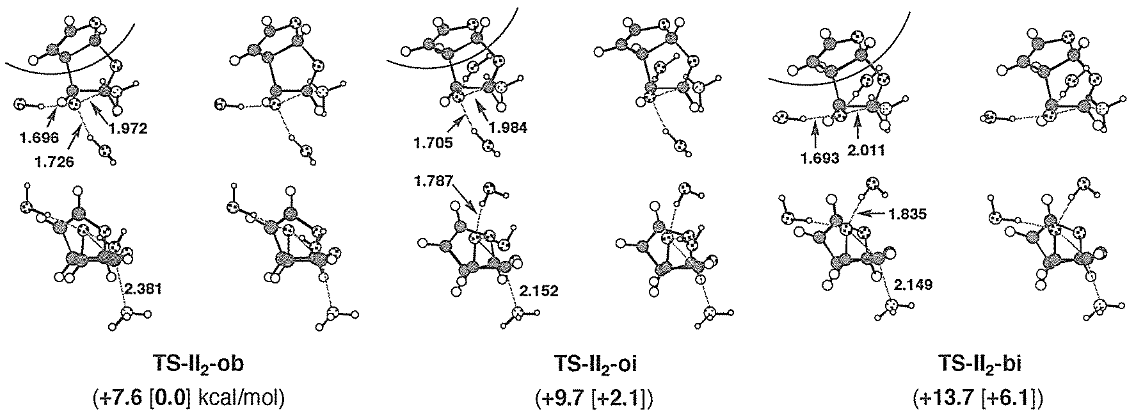

Fig.3 Stereoviews of RHF/3-21G transition structures for S_N2 type nucleophilic oxirane ring opening of endo type model compound (**II**) by NH_3. Two H_2O molecules coordinate to oxirane oxygen, on which negative charge grows as the reaction proceeds. Three types of coordinating geometries could be located, which are designated as **TS-II$_2$-ob**, **TS-II$_2$-oi**, and **TS-II$_2$-bi**. Atomic distances are in angstroms. Energy differences are at Becke3LYP/3-21G//RHF/3-21G and are the ones between the corresponding transition structure and **TS-I$_2$** shown in Fig. 2.

Becke3LYP/6-31G*//RHF/6-31G* level is almost the same (8.8 kcal/mol).

Figs. 2 and 3 show stereoviews of two endo-attacking TSs (**TS-I$_2$** and **TS-I'$_2$**) and three exo-attacking TSs (**TS-II$_2$-ob**, **TS-II$_2$-oi**, and **TS-II$_2$-bi**), respectively, located at the RHF/3-21G basis set. The symbol "**ob**" in "**TS-II-ob**" means the coordination of two H_2O molecules from outside and backside direction, "**oi**" from outside and inside, and "**bi**" from backside and inside (Fig. 4). The subscript "**2**" indicates the number of coordinating H_2O molecules. The most stable endo-attacking **TS-I$_2$** has the geometry that oxygen of inside H_2O coordinates to two C-H hydrogen atoms. **TS-I'$_2$** has a single C-H...O contact and is slightly less stable (by 1.6 kcal/mol at Becke3LYP/3-21G//RHF/3-21G) than **TS-I$_2$**. Three **TS-IIs** shown in Fig. 3 have the geometries, which five-membered B ring faces with oxirane ring, and therefore, solvation by H_2O must occur

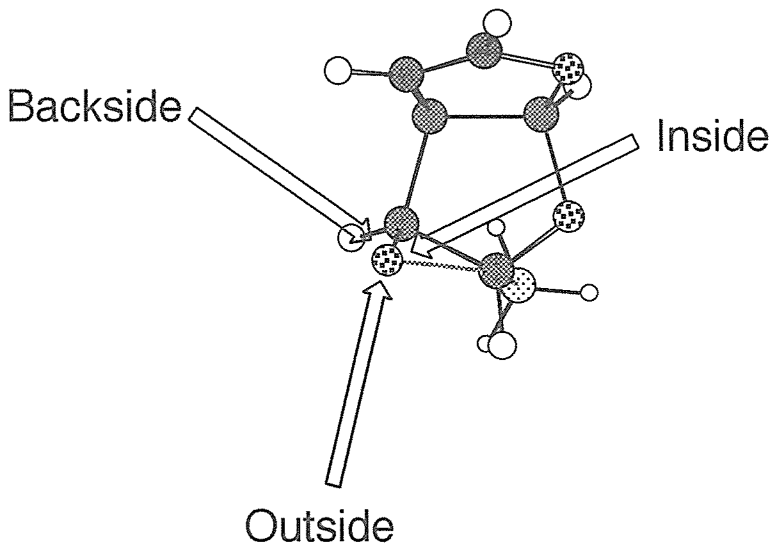

Fig.4 The direction of coordination of solvent molecules to oxirane oxygen.

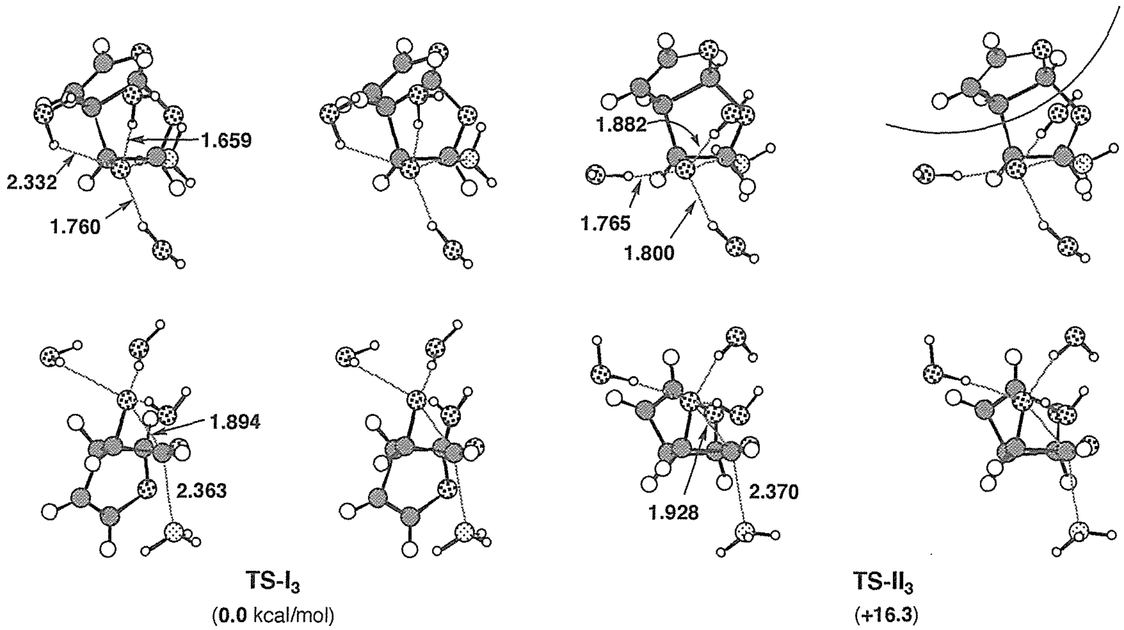

Fig.5 Stereoviews of RHF/3-21G transition structures for S_N2 type nucleophilic oxirane ring opening of model compounds (**I** and **II**) by NH_3 molecule. Three H_2O molecules coordinate to oxirane oxygen, on which negative charge grows as the reaction proceeds. Single transition structure (TS-I_3 for **I** and TS-II_3 for **II**, respectively) could be located. Atomic distances are in angstroms. Energies are at Becke3LYP/3-21G//RHF/3-21G.

Table1. Activation energies ($\Delta E^{\neq}$, kcal/mol) evaluated at Becke3LYP/3-21G//RHF/3-21G level.

no H_2O		$(H_2O)_n$, n=2					$(H_2O)_n$, n=3	
exo	endo	exo (endo attack)		endo (exo attack)			exo	endo
TS-I	**TS-II**	**TS-I$_2$**	**TS-I'$_2$**	**TS-II$_2$-ob**	**TS-II$_2$-oi**	**TS-II$_2$-bi**	**TS-I$_3$**	**TS-II$_3$**
+24.4	+32.2	**+9.7**	+11.4	**+14.3**	+16.4	+20.4	**+7.4**	+20.5

from the side of B ring. The most stable exo-attacking TS is **TS-II2-ob** and is followed by **TS-II2-oi** (+2.1 kcal/mol) and **TS-II2-bi** (+6.1). **TS-II2-ob** is less stable by +7.6 kcal/mol than the most stable endo-attacking **TS-I2**. The relative energies also shown in Figures 2 and 3 implies that endo attacking is predominant to exo attacking. Activation energies ($\Delta E^{\neq}$) were evaluated to be only +9.7 kcal/mol for **TS-I2**. On the other hand, $\Delta E^{\neq}$ value for **TS-II2-ob** is +14.3 kcal/mol (Table 1). The coordination of two H_2O molecules at the oxirane oxygen atom, on which negative charge grows as the C-O bond breaking proceeds, considerably reduces $\Delta E^{\neq}$ values as compared with the case considering no solvent molecule (Fig. 1). Although the stabilization of TS by the solvent effect is considered to be mainly obtained by Coulomb stabilization between growing negative charge on oxirane oxygen and coordinated H_2O, exo-attacking TSs (**TS-IIs**) must suffer severe steric congestion between B ring (coumarin ring of AFB_1 8,9-oxide (**1**)) and coordinating H_2O molecules. Actually, less stable **TS-II2-oi** and **TS-II2-bi** include the most sterically unfavorable inside coordination of H_2O. It is concluded that the solvation by H_2O could stabilize TSs in the order of **ob** > **oi** > **bi** coordination mode. The critical geometrical

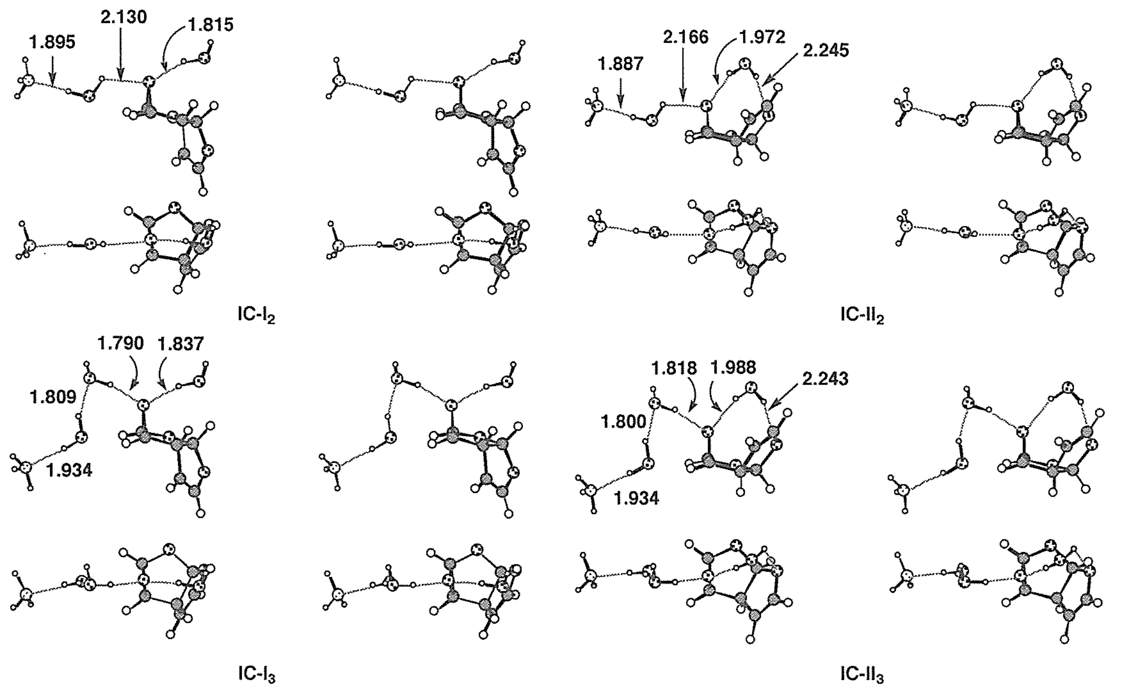

Fig.6 Stereoviews of RHF/3-21G geometries of initial complexes (**ICs**). Atomic distances are in angstroms.

parameters at transition state indicate that the most stable **TS-II2-ob** is the earliest of the three and the least stable **TS-II2-bi** latest (atomic distances are in order of 2.381 Å, 2.152, and 2.149 for forming C...N and 1.972, 1.984, 2.011 for breaking C...O for **TS-II2-ob**, **TS-II2-oi**, and **TS-II2-bi**, respectively) and the $\Delta E^{\neq}$ values of these TSs increase as TSs become later.[11]

Fig. 5 shows the stereoviews of RHF/3-21G TSs (**TS-I3** for the reaction of **I** and **TS-II3** for **II**) having three H_2O molecules coordinated to oxirane oxygen. Only one TS could be located for the reaction of each reactant. $\Delta E^{\neq}$ values for **TS-I3** and **TS-II3** could be evaluated to be +7.4 and +20.5 kcal/mol at Becke3LYP/3-21G//RHF/3-21G level (Table 1). As shown in Table 1, **TS-I3** has the smallest $\Delta E^{\neq}$ value in all endo-attacking TSs studied here, probably because of larger coordination space around exo positioned oxirane oxygen and the fact that non-congested coordination of maximum three H_2O molecules is possible in endo-attacking TS. On the other

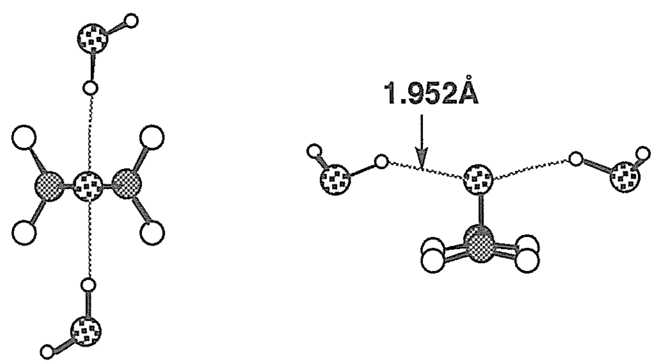

Fig.7 Becke3LYP/6-31G* structure of ethylene oxide coordinated by two H_2O molecules.

hand, **TS-II$_2$-ob** has the least $\Delta E^{\neq}$ (+14.3 kcal/mol) in the series of exo-attacking TSs. **TS-II$_3$** (+20.5 kcal/mol) having three coordinating H_2O has larger $\Delta E^{\neq}$ (by 6.3 kcal/mol) than that of **TS-II$_2$-ob**. Clearly, there exists severe steric repulsion between B ring and two H_2O molecules in **TS-II$_3$**. Actually, $\Delta E^{\neq}$ values of **TS-II$_3$** (+20.5 kcal/mol) and **TS-II$_2$-bi** (+20.4 kcal/mol) is quite the same, indicating that these large $\Delta E^{\neq}$s are caused mainly by inside coordination of H_2O.

These results imply that **TS-I$_3$** could be favorably stabilized by the hydrogen bonding between growing negative charge on oxirane oxygen and three H_2O solvents, however, the repulsive interaction between backside and inside H_2O solvent molecules and B ring offsets Coulomb stabilization obtained by hydorgen bonding between oxirane oxygen and them.

Finally, Fig. 6 shows stereoviews of RHF/3-21G geometries of initial complexes (**ICs**). In **ICs**, no stable structures having three H_2O molecules coordinated to oxirane oxygen could be located. It seems that negative charge on oxirane oxygen is too small to make hydrogen bonding with three H_2O molecules, considering the fact that hydrogen bonding with only two H_2O is possible. The coordination of two H_2O toward oxirane oxygen occurs from the direction which each set of lone pair electrons spreads out, in spite of the steric hindrance of two C-H bond in **I** and B ring in **II**. The groud state geometry located at Becke3LYP/6-31G* level for two H_2O coordinating structure to oxygen atom of ethylene oxide is shown in Fig. 7. Two H_2O molecules also coordinate to oxirane oxygen from the same direction seen in these **ICs**. It is likely that the maximum stabilization energy could be obtained by this coordination mode in the solvation by two H_2O molecules toward oxirane oxygen. Any ground state structure having three H_2O molecules coordinated to oxirane oxygen of ethylene oxide could not be located at Becke3LYP/6-31G* level, in spite of little steric hindrance around oxirane oxygen.

Summary

In order to investigate the solvation effect of S_N2 type nucleophilic oxirane ring opening of AFB_1 8,9-oxide (**1**), *ab initio* molecular orbital calculation for the model reaction of **I** and **II** with NH_3 molecule was performed. The solvation by nH_2O molecules (n=2-3) around oxirane oxygen, on which negative charge grows as the reaction proceeds, was considered. Calculation clarified the following points: (1) involvement of the solvent molecules accelerate the reaction. (2) $\Delta E^{\neq}$ values (+24.4 kcal/mol (**TS-I**), +9.7 (**TS-I$_2$**), and +7.4 (**TS-I$_3$**)) for the reaction of **I** are generally smaller than those (+32.2 (**TS-II**), +14.3 (**TS-II$_2$-ob**), and +20.5 (**TS-II$_3$**)) for **II**, suggesting that endo-attacking process is more favorable than exo-attacking one. (3) For endo-attacking TSs, $\Delta E^{\neq}$ value of **TS-I$_3$** (+7.4kcal/mol) coordinated by three H_2O molecules is the smallest, while **TS-II$_2$-ob** with two H_2O has the smallest $\Delta E^{\neq}$ value in the series of exo-attacking TSs. (4) For exo-attacking TSs, three direction (outside (**o**), backside (**b**), and inside (**i**)) for solvent coordination is possible and steric hindrance increases in the order of **o**< **b**< **i** (net stabilization obtained by solvation is in the order of **o** >**b** >**i**). The solvent effect found in the reaction of **I** and **II** implies that coumarin skeleton in AFB_1 8,9-oxide (**1**) might give more serious steric influence for the solvation of exo-attacking TSs.

References

1) Groopman, J. D., Cain, L. G.; Kensler, T. W. *Crit. Rev. Toxicol.*, **19**, 113 (1988): Busby, W. F., Wogan, G. N. In *Chemical Carcinogens*; Searle; C.E., Ed.; American Chemical Society: Washington, DC, 1984; pp. 945-1136: Garner, R. C., Wright, C. M. *Br. J. Cancer*, **28**, 544 (1973): Detroy, R. W.; Lillehoj, E. B.; Ciegler, A. In *Microbial Toxins*, Ciegler, A.; Kadis, S.; Ajl, S. J., Ed.; Academic Press, New York, 1971; Vol. 6, pp. 3-178.
2) Massey, T. E., Stewart, R. K., Daniels, J. M., Liu, L. *Proc. Exp. Biol. Med.*, **208**, 213 (1995).
3) Ueng, Y-F., Shimada, T., Yamazaki, H., Guengerich, F. P. *Chem. Res. Toxicol.* **1995**, 8, 218: Shimada, T., Guengerich, F. P. *Proc. Natl. Acad. Sci. U. S. A.*, **86**, 462 (1989).
4) Raney, V. M., Harris, T. M., Stone, M. P. *Chem. Res. Toxicol.*, **6**, 64 (1993).
5) Iyer, R.; Coles, B., Raney, K. D. Thier, R., Guengerich, F. P., Harris, T. M. *J. Am. Chem. Soc.*, **116**, 1603 (1994).
6) (a) M. Bonnett, E. R. Taylor, *J. Biomol. Struct. Dyn.*, **7**, 127 (1989); (b) A. C. Pavao, L. A. S. Neto, J. F. Neto, M. B. C. Leao, THEOCHEM, **337**, 57 (1995); R. Pachter, P. S. Steyn, *Mutat. Res.*, **143**, 87 (1985).
7) Gaussian 98, Revision A.4, M. J. Frisch, G. W. Trucks, H. B. Schlegel, G. E. Scuseria, M. A. Robb, J. R. Cheeseman, V. G. Zakrzewski, J. A. Montgomery, Jr., R. E. Stratmann, J. C. Burant, S. Dapprich, J. M. Millam, A. D. Daniels, K. N. Kudin, M. C. Strain, O. Farkas, J. Tomasi, V. Barone, M. Cossi, R. Cammi, B. Mennucci, C. Pomelli, C. Adamo, S. Clifford, J. Ochterski, G. A. Petersson, P. Y. Ayala, Q. Cui, K. Morokuma, D. K. Malick, A. D. Rabuck, K. Raghavachari, J. B. Foresman, J. Cioslowski, J. V. Ortiz, B. B. Stefanov, G. Liu, A. Liashenko, P. Piskorz, I. Komaromi, R. Gomperts, R. L. Martin, D. J. Fox, T. Keith, M. A. Al-Laham, C. Y. Peng, A. Nanayakkara, C. Gonzalez, M. Challacombe, P. M. W. Gill, B. Johnson, W. Chen, M. W. Wong, J. L. Andres, C. Gonzalez, M. Head-Gordon, E. S. Replogle, and J. A. Pople, Gaussian, Inc., Pittsburgh PA, 1998.
8) Energies (Becke3LYP/3-21G//RHF/3-21G) and single imaginary frequency (in parenthesis) for RHF/3-21G TSs (cm^{-1}) are as follows: Transition structures (TSs); **TS-I**, -511.508792 (-472.0); **TS-II**, -511.494898 (-371.7); **TS-I$_2$**, -663.536437 (-368.4); **TS-I'$_2$**, -663.533800 (-395.7); **TS-II$_2$-ob**, -663.524263 (-275.0); **TS-II$_2$-oc**, 663.520876 (-378.7); **TS-II$_2$-bc**, -663.514548 (-349.9); **TS-I$_3$**, -739.548984 (-370.6); **TS-II$_3$**, -739.522898 (-318.7).
   Initial Complexes (ICs); **IC-I**, -511.547618; **IC-II**, -511.546252; **IC-I$_2$**, -663.551971; **IC-II$_2$**, -663.547023; **IC-I$_3$**, -739.560798; **IC-II$_3$**, -739.555505.
9) Schlegel, H. B. In *Encyclopedia of Computational Chemistry*, Schleyer, P. v. R., Ed. in chief, vol. 4, pp. 2432, John Wiley & Sons Ltd. (1998).
10) Activation energies ($\Delta E^{\neq}$) were calculated to be the energy difference between the TSs (Figures 2-3 and 5) and the corresponding initial complexes shown in Fig. 6.
11) Pross, A. In *Advances in Physical Organic Chemistry*, vol. 14, pp. 73, Academic Press (1977).